

# Laterally Confined Modes in Wet-Etched, Metal-Coated, Quantum-Dot-Inserted Pillar Microcavities \*

ZHANG Hao(章昊)<sup>1\*\*</sup>, ZHENG Hou-Zhi(郑厚植)<sup>1</sup>, ZHANG Ji-Dong(章继东)<sup>1</sup>, XU Ping(徐萍)<sup>1</sup>,  
TAN Ping-Heng(谭平恒)<sup>1</sup>, YANG Fu-Hua(杨富华)<sup>1</sup>, ZENG Yi-Ping(曾一平)<sup>2</sup>

<sup>1</sup>State Key Laboratory of Superlattices and Microstructures, Institute of Semiconductor, Chinese Academy of Sciences,  
PO Box 912, Beijing 100083

<sup>2</sup>Novel Material Department, Institute of Semiconductor, Chinese Academy of Sciences, PO Box 912, Beijing 100083

(Received 16 September 2003)

*We report the fabrication and the measurement of microcavities whose optical eigenmodes were discrete and were well predicted by using the model of the photonic dot with perfectly reflected sidewalls. These microcavities were consisted of the semiconductor pillar fabricated by the simple wet-etched process and successive metal coating. Angle-resolved photoluminescence spectra demonstrate the characteristic emission of the corresponding eigenmodes, as its pattern revealed by varying both polar ( $\theta$ ) and azimuthal ( $\Phi$ ) angles. It is shown that the metal-coated sidewalls can provide an efficient way to suppress the emission due to the leaking modes in these pillar microcavities.*

PACS: 42.50.Ct, 71.36.+c, 78.66.Fd

In a laterally confined semiconductor microcavity, made from planar microcavities by nanofabrication technology, both the longitudinal confinement by top and bottom distributed Bragg reflectors (DBR) and the waveguiding by sidewalls play an important role for allowing the pillar microcavity to sustain a discrete set of three-dimensionally (3D) confined optical modes.<sup>[1-3]</sup> Such pillar microcavity reduces the number of allowed modes, but increases the mode density of these resonant modes, giving rise to enhanced or suppressed spontaneous emission in the so-called weak coupling regime.<sup>[4-7]</sup> This cavity quantum electrodynamics (CQED) phenomenon has been employed to exploit high-efficiency light-emitting diodes for optical communications and single photon sources for quantum cryptography.<sup>[8,9]</sup> Still, the enhancement of the spontaneous emission is mainly determined by the Purcell factor  $F_p = 3Q\lambda^3/4\pi V$ ,<sup>[5]</sup> where  $Q$  is the cavity finesse,  $\lambda$  is the transition wavelength, and  $V$  is the cavity mode volume. However, in order to make the spontaneous emission coupling coefficient  $\beta$  close to one, defined as the fraction of total spontaneous emission from the internal light emitters captured into the fundamental cavity modes, the suppression of leaking modes in the pillar microcavity also appears to be a key factor. Since DBRs have a high reflection coefficient only within a limited angle stop-band,<sup>[10]</sup> the portion of spontaneous emission from quantum wells (QWs) or quantum dots (QDs),<sup>[11]</sup> which shines internally on the DBRs or sidewalls at an angle larger than the above critical angle, will inevitably be lost in quasi-continuum leaking modes. With reducing the

lateral size of the pillar microcavity, the coupling of the spontaneous emission into the leaking modes becomes even more severe. By coating its sidewall with metal, a pillar microcavity showed an effective suppression of leaky modes.<sup>[6]</sup> However, one is not clear that to what extent the electromagnetic field pattern of the cavity mode might vary in such coated pillar microcavity, as compared to that of uncoated one.

In the present work, we report discretized optical eigenmodes<sup>[14]</sup> in QDs inserted semiconductor-pillar-microcavities with the lateral size of  $4.1\ \mu\text{m}$  in radius. Although, these pillar microcavities show rather tapered sidewalls in their shapes due to the wet etching process, our spectrum measurements have shown that aluminum-coated sidewalls of the pillar microcavities can efficiently suppress the leaking modes. However, the leading high order modes, even like (006), could still show up. The far-field emissions detected at different angles proven that the eigenenergies of these laterally confined modes were all in a good agreement with the values predicted for a photonic dot with a perfectly reflected sidewall. The angle-resolved photoluminescence also demonstrated the characteristic emission patterns for different eigenmodes, as revealed by varying polar ( $\theta$ ) and azimuthal ( $\Phi$ ) angles.<sup>[12]</sup>

The microcavity structure in use (see Fig. 1) was grown on an undoped (100) GaAs substrate by molecular beam epitaxy (MBE). A cavity spacer of nominal length  $L_c = 3/2\ \lambda = 442\ \text{nm}$  was sandwiched between the bottom and top distributed Bragg reflectors (DBRs), which consist of 19-period and 15-period quarter-wave layers, using GaAs/AlAs respec-

\* Supported by the Major State Basic Research Project of China (G001CB3095), the Special Project from Chinese Academy of Sciences, and the National Natural Science Foundation of China under Grant No 60076026.

\*\* Email: zhanghao@red.semi.ac.cn

©2004 Chinese Physical Society and IOP Publishing Ltd

tively. AlAs and GaAs layers in the DBRs were of 83.9 nm and 73.6 nm in thickness, respectively. Two groups of three stacked layers of self assembled  $\text{In}_{0.5}\text{Ga}_{0.5}\text{As}$  QDs (each was formed by 4 monolayers of  $\text{In}_{0.5}\text{Ga}_{0.5}\text{As}$ ) were located at two antinodes<sup>[13]</sup> of the planar cavity. All the layers were grown at 600°C except the QDs with the growing temperature lowered to 500°C. The central wavelength of the stopband is designed to be 1060 nm by selecting the refraction index,  $n_1 = 3.58$  for GaAs and  $n_2 = 2.96$  for AlAs. The reference sample for the photoluminescence (PL) measurement at 77 K was centered at 992 nm, consisting of only self-assembled  $\text{In}_{0.5}\text{Ga}_{0.5}\text{As}$  QDs in the GaAs matrix and being grown at the same temperature. The obtained planar microcavity exhibits typically a high finesse factor  $Q$  of 2000, as characterized by photoreflexion spectrum. To obtain three-dimensional photon confinements, arrays of circular photonic dots were fabricated by conventional photolithography and wet

etching. One may notice that the actual shape of the etched pillar was apart slightly from the circle. On the top of the pillar an optical aperture of 1.5  $\mu\text{m}$  in size (not shown in Fig. 1(b)) was then opened by photolithography for light access.

The samples were mounted in a liquid-nitrogen (77 K) cryostat. The light beam of a He-Ne laser (632.8 nm) was steered into the optical aperture from top of the pillar. The emitted light was dispersed by the Dilor SuperLabram monochrometer, and detected by a liquid-nitrogen-cooled CCD detector. Through a TV camera, we can clearly see every single pillar microcavity, the little laser-beam spot and some alignment marks for photolithography on the chip. Using these marks, we can recognize every specific pillar microcavity on the chip. Since the spatial interval between pillars was about 100  $\mu\text{m}$  that was much larger than the laser-beam spot size ( $\sim 1 \mu\text{m}$ ), the measured emission is surely from an individual pillar microcavity.

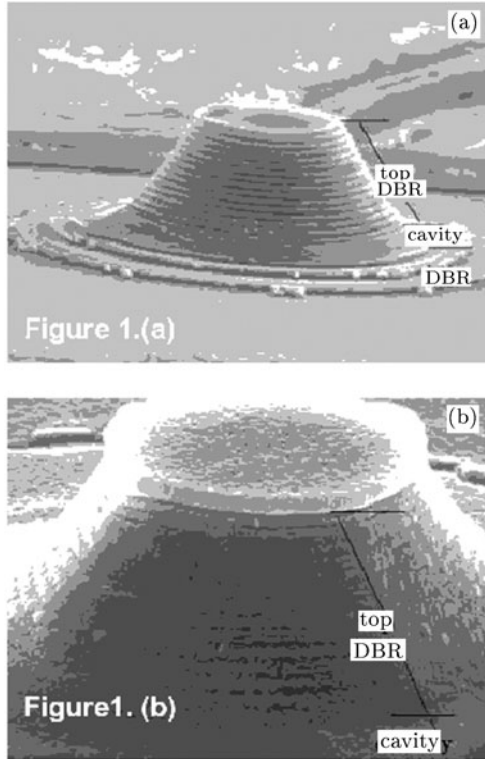


**Fig. 1.** Scanning electron micrographs of a wet-etched pillar microcavity (a) without Al-coating or (b) with Al-coating.

etching. The laterally patterned structures were unselectively etched, starting from the top DBR, going through the cavity layer and eventually down to few pairs of the bottom DBR using a phosphoric-acid-based solution ( $\text{H}_3\text{PO}_4:\text{H}_2\text{O}_2:\text{H}_2\text{O}=3:0.5:1$ ) held at a temperature of  $20 \pm 0.1^\circ\text{C}$ . Figure 1(a) shows the scanning electron micrograph (SEM) of a pillar microcavity. Then, the pillar microcavity was fully covered with 100 nm-thick aluminum by evaporation as seen

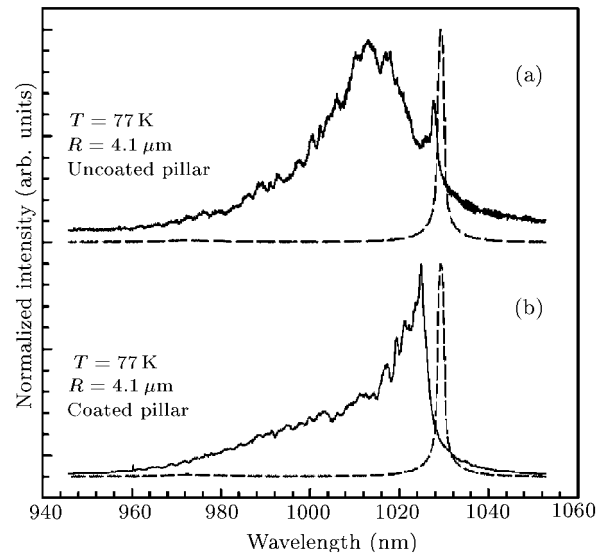


**Fig. 2.** Wide-angle-collected PL spectra of a wet-etched pillar microcavity (a) without Al-coating or (b) with Al-coating. The dotted line is the PL spectrum of the counterpart of a planar microcavity.

Figure 2(a) shows the PL spectrum of an uncoated pillar microcavity with 4.1  $\mu\text{m}$  in radius, detected by a wide-angle collection. For the sake of comparison, the PL spectrum of the unpatterned planar microcavity is also shown in the figure by the dotted line. The broaden PL background without any spectral features resembles closely to that of the naked self-assembled  $\text{In}_{0.5}\text{Ga}_{0.5}\text{As}$  QDs in GaAs matrix. The sharp peak at 1028 nm is assigned to the fundamental cavity mode, which is blue shifted from the counter part (1030 nm) of the planar microcavity. It is very obvious that a large portion of QD emission is lost in quasi-continuous leaking modes. The

situation became even worse in our wet-etched pillar microcavity. The isotropic wet-etching made the sidewalls more tapered. A significant part of QDs was in fact naked without any confinement in the vertical direction due to the destroying of the top DBR near the edge. Displayed in Fig. 2(b) is the PL spectrum of a coated pillar microcavity. As compared to Fig. 2(a), the emission through the leaking modes was greatly suppressed, while the intensity of the fundamental cavity mode was enhanced with its peak blue-shifted. Thus, we are convinced of the effectiveness in eliminating the emission through the leaking modes by metal-coating the sidewalls of the wet-etched pillar microcavities. Also, we have measured several pillars. The result shows that the measurement was repeatable.

To identify clearly high order cavity modes and obtain the information about the electromagnetic field distribution in the coated pillar microcavity, we have performed angle resolved PL spectra. The cryostat was mounted on a translation platform, which could be rotated with respect to the collection lens. In front of the lens, an optical aperture was inserted so that a light hole of 0.6 mm in radius located away from the sample by a distance of 30 mm to ensure an angle detection resolution of about  $1^\circ$ . A certain cavity mode has its characteristic far-field emission-pattern around certain spatial direction  $(\theta, \Phi)$ .<sup>[3]</sup> Our cavity modes should appear more pronounced by the angle-resolved PL spectra than by wide-angle collection. Moreover,

the emission intensity from each cavity mode may vary by changing the detection angle  $(\theta, \Phi)$ . This makes the assignment of the different cavity modes further confirmed in the angle-resolved PL spectra. Figure 3 gives angle-resolved spectra of a pillar microcavity with a size of  $4.1 \mu\text{m}$  in radius at a fixed azimuthal angle  $\Phi = 0^\circ$  (a),  $\Phi = 45^\circ$  (b). The spectrum, measured at the different polar angle  $\theta$  in a range from  $0^\circ$  to  $18.4^\circ$ , is offset along the vertical axis for clarity. The mode index is denoted by  $(n_r, n_\phi, n_z)$ . As is seen, several laterally confined cavity modes appear on the short-wavelength side of the fundamental mode. Their intensity variation was measured by changing polar angle  $\theta$ , while some of these modes were disappeared at certain  $\theta$  angles. However, the location of their peaks did not vary with  $\theta$ , which led to the evidence of the laterally confined cavity modes. To assign the cavity modes, the eigenenergies of three-dimensionally confined cavity modes can just simply be given by<sup>[2]</sup>

$$E_{ph} = \sqrt{E_0^2 + \frac{\hbar^2 c^2}{\varepsilon} \frac{x_{n_\phi, n_r}^2}{R^2}}$$

for a metal-coated pillar microcavity since the reflectivity of its sidewall tends to unity. Here  $E_0 = \hbar c k_z / n$  denotes the energy of the unetched cavity with  $k_z = 2\pi n / \lambda_0$  being the corresponding wave vector;  $x_{n_\phi, n_r}$  is the  $n_r^{\text{th}}$  zero of the Bessel function  $J_{n_\phi}(x_{n_r, n_\phi} r / R)$ ,  $R$  is the radius of the circular dot.

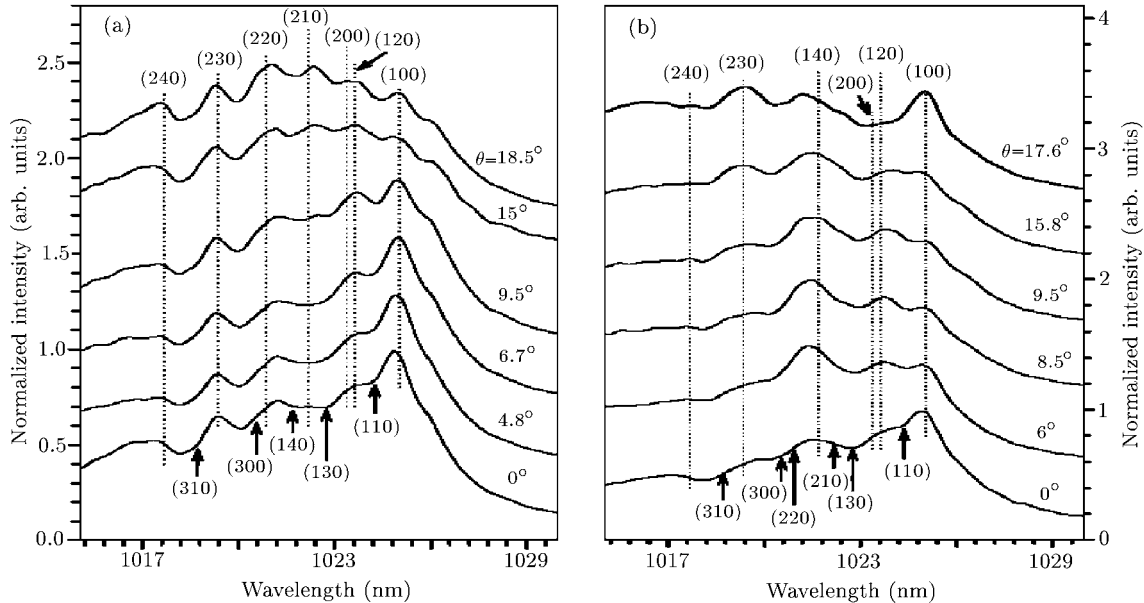


**Fig. 3.** Angle-resolved spectra of an Al-coated pillar microcavity with a lateral size of  $R = 4.1 \mu\text{m}$ , in which the polar angle  $\theta$  was tuned from 0 to  $18.4^\circ$  for a fixed azimuthal angle (a)  $\Phi = 0^\circ$  or (b)  $\Phi = 45^\circ$ . The dotted vertical lines denoted the energies of eigenmodes  $(n_r, n_f, n_z)$  predicted for a photonic dot with perfectly reflected sidewall. Short arrows indicate the missing modes.

The calculated values of the mode energies are also indicated by the vertical lines in Fig. 3, with  $R = 4.1 \mu\text{m}$  and  $n = 3.58$  being used. One may find that the measured spectrum peaks in a range from 1015 nm to 1025 nm are in good agreement with the calculated modes. By a close look of Fig. 3(a), however, one also knows that the modes (200) and (120) are too close to be resolved in the measured spectra. In addition, compared with the calculated mode spectra, many modes (e.g., (110), (130), (140), (300) and (310)) are missing in the PL spectra for  $\Phi = 0^\circ$  as denoted by the short arrows in Fig. 3(a). On the other hand, it is intrigued to notice that for  $\Phi = 0^\circ$  the mode (210) is in absence as  $\theta \leq 6.7^\circ$ , and appears with the increasing polar angle from  $\theta > 9.5^\circ$ , while the PL intensity of the mode (100) at  $\Phi = 0^\circ$  has its maximum, and decreases with increasing  $\theta$  monotonously. By turning azimuthal angle  $\Phi$  to  $45^\circ$ , the spectra in Fig. 3(b) show somewhat different behaviour. This may be attributed to the fact that the actual shape of the etched pillar deviates from the perfect circle, enforced by nonisotropic wet etching as revealed by Fig. 1(b). First, the mode (240) becomes hardly discernible. Secondly, the mode (100) has its first maximum intensity at  $\theta = 0^\circ$ , decreases with increasing  $\theta$  up to  $9.5^\circ$  and increases again at  $\theta = 17.6^\circ$ . Thirdly, the mode (220) is missing at  $\Phi = 45^\circ$ , instead a new mode (140) appears. It is well known that<sup>[3]</sup> the dependence on the spatial direction angle ( $\theta, \Phi$ ) of the far-field emission from a pillar microcavity is determined by the Fourier transform of the electromagnetic field in the cavity plane. At a certain solid angle only selected cavity modes can emit into it with appreciable intensity. This forms the physical origin for the phenomena observed in Fig. 3. However, the details of the intensity variation between the different cavity modes and their dependences on the detection angle are also related to the randomness nature of self-assembled QDs. At a certain detection angle, only those QDs, which are both well matched spectrally with the allowed cavity modes and located close to the cavity antinodes, make the contribution to the PL. This fact will contribute to the fluctuation further. Missing modes might partially due to

their corresponding reduction on the finesse factor of the pillar microcavity, which should be further deteriorated by laterally patterning. However, it is clear that the field distribution in our wet-etched pillar microcavity certainly plays an important role for their absence at certain solid angles.

In summary, discretized optical eigenmodes in wet-etched, metal-coated pillar microcavities, with a radius size of  $4.1 \mu\text{m}$ , have been reported in a good agreement with that predicted for a photonic dot with a perfectly reflected sidewall. The angle-resolved PL spectra demonstrate the characteristic emission patterns for different eigenmodes, as revealed by varying both polar ( $\theta$ ) and azimuthal ( $\Phi$ ) angles. It is also proven that the metal-coating on the sidewall provides an efficient way to suppress the emission through the leaking modes.

## References

- [1] Reithmaier J P, Röhner M, Zull H, Schäfer F, Forchel A, Knipp P A and Reinecke T L 1997 *Phys. Rev. Lett.* **78** 378
- [2] Gutbrod T, Bayer M, Forchel A, Reithmaier J P, Reinecke T L, Rudin S and Knipp P A 1998 *Phys. Rev. B* **57** 9950
- [3] Gutbrod T, Bayer M, Forchel A, Knipp P A, Reinecke T L, Tartakovskii A, Kulakovskii V D, Gippius N A and Tikhodeev S G 1999 *Phys. Rev. B* **59** 2223
- [4] Ohnesorge B, Bayer M, Forchel A, Reithmaier J P, Gippius N A and Tikhodeev S G 1997 *Phys. Rev. B* **56** R4367
- [5] Gérard J M, Sermage B, Gayral B, Legrand B, Costard E and Thierry-Mieg V 1998 *Phys. Rev. Lett.* **81** 1110
- [6] Bayer M, Reinecke T L, Weidner F, Larionov A, McDonald A and Forchel A 2001 *Phys. Rev. Lett.* **86** 3168
- [7] Solomon G S, Pelton M and Yamamoto Y 2001 *Phys. Rev. Lett.* **86** 3903
- [8] Kim J, Benson O, Kan H and Yamamoto Y 1999 *Nature* **397** 500
- [9] Imamoglu A, Schmidt H, Woods G and Deutsch M 1997 *Phys. Rev. Lett.* **79** 1467
- [10] Panzarini G, Andreani L C, Armitage A, Baxter D, Skolnick M S, Astratov V N, Roberts J S, Kavokin A V and Vladimirova M R 1999 *Phys. Rev. B* **59** 5082
- [11] Liu W K, Lin S M and Zhang C S 2002 *Chin. Phys. Lett.* **19** 843
- [12] Zhao J M, Ma F Y, Liu X Y, Liu Y, Chu G Q, Ning Y Q and Wang L J 2002 *Chin. Phys. Lett.* **19** 1447
- [13] Zhang J T, Feng X L, Zhang W Q and Xu Z J 2002 *Chin. Phys. Lett.* **19** 670
- [14] Cheng T W et al 2002 *Chin. Phys. Lett.* **19** 1792